Universidad del País Vasco
Euskal Herriko Unibertsitatea
ZIENTZIA ETA TEKNOLOGIA FAKULTATEA
FACULTAD DE CIENCIA Y TECNOLOGÍA

Final Degree Thesis
Double Degree in Physics and Electronic Engineering (Physics Thesis)

Study on the photoluminescence of 2D metal-halide perovskite materials

Author:
Luis Arriola Carril
Supervisors:
Prof. Dr. José María Pitarke De La Torre
Dr. Beatriz Martín García

Leioa, 22nd June 2022

Abstract

Hybrid organic-inorganic metal halide perovskites have emerged as promising materials in the development of optoelectronic devices, namely due to their high optical absorption coefficient, tuneable bandgap and charge carrier mobility. However, more efforts are needed to improve their stability against oxygen, moisture and light and find new ways to modulate their optical properties. In this work, we study the photoluminescence properties of lead-bromide-based layered (2D) perovskites with different composition and dimensionality as bulk crystals and mechanically exfoliated flakes. We highlight the tuning of the photoluminescence emission of 2D metal halide perovskites by design and enhance their ambient stability by encapsulating the exfoliated flakes with h-BN flakes. Finally, we carry out the fabrication of heterostructures using as building blocks perovskite flakes showing how to further modulate the photoluminescence emission colour.

Contents

1 Introduction **4**

1.1 Crystal structure of the metal-halide perovskites 4

1.1.1 Layered perovskites 4

1.2 Optoelectronic properties of metal-halide perovskites 5

1.3 Interest and challenges 6

1.4 Objectives of the study 6

2 Experimental techniques **8**

2.1 Exfoliation procedure 8

2.2 Dry viscoelastic stamping system 9

2.3 Micro photoluminescence spectroscopy 10

2.4 Atomic Force Microscopy 11

3 Results and discussion **12**

3.1 Characterization of the materials: bulk and flakes 12

3.1.1 Absorption and photoluminescence spectra of bulk crystals 12

3.1.2 Characterization of perovskite flakes 14

3.2 Stability study 18

3.2.1 Exposure to the atmosphere 18

3.2.2 Exposure to light 23

3.3 Building heterostructures 29

3.3.1 Effect of the order of the stack 29

3.3.2 Effect of an hBN barrier 31

3.3.3 Effect of flake thickness 32

4 Conclusions **35**

1 Introduction

The need of novel solutions in optoelectronics materials for application in light emitting diodes (LEDs), phosphors, scintillators and photodetectors has been a driving force in nanomaterials research for the past years. Efforts have been focused to improve properties such as emission or absorption efficiency, control and tunability of the spectral features (from narrow, pure color to broad, nearly-white emission), modulation of the emission with external knobs, response speed and sensitivity. In the last years, the metal halide perovskites have awakened the attention of the scientific community as a new class of materials for the development of the next-generation of optoelectronic devices. The 3D metal halide perovskites stand out in the photovoltaic applications. Since the first solar cell with a power conversion efficiency (PCE) of 3.81% nowadays achieve more than 25%[1].However, going a step further, the dimensional reduction of 3D perovskites toward layered structures can boost the photoluminescence quantum yield (PLQY) and expand their emission range for other optoelectronic applications[2], e.g. as blue-LEDs, PLQY of 88% together with stable emission under high operation voltages and a maximum luminance of 2480 cd m^{-2} has been achieved[3]. However, there are still some challenges to be addressed in this area and in which we focus this work: (i) the modulation of the photoluminescence emission and (ii) the development of strategies to enhance their stability against moisture, oxygen or light[4,5].

1.1 Crystal structure of the metal-halide perovskites

The perovskite structure has been known since the XIX century, with the $CaTiO_3$ mineral discovered by Gustav Rose and is named after Russian noble and mineralogist Lev Alekseyevich von Perovski. The general formula of the perovskite structure is ABX_3. They consist of divalent B-site cations surrounded by anions (X) that create a corner-sharing octahedra network, with A-site monovalent cations that occupy the cavities of the octahedral network. In the particular case of metal halide perovskites, studied in this work, A is an inorganic or small organic monovalent cation (such as Cs or methylammonium, MA), B is a metal cation and X is a halide anion (Cl, Br, I). To this date and regarding the metal site, remarkable good properties have been obtained with Pb, but there is a large library of perovskites, including Sn, Ge, Cd, and Mn, for instance[5].

1.1.1 Layered (two-dimensional) perovskites

The layered metal-halide perovskites consist on replacing the small A-site cation in the 3D structure detailed before by large organic cations. In this way a quasi-2D structure is obtained, where each layer of octahedra is separated by organic layers. There are two type of phases depending on the organic cations used: Ruddlesden-Popper (RP) and Dion-Jacobson (DJ). While the RP phase contains two monoammonium cations, the DJ phase contains diammonium cations[6]. However, we this study on RP perovskites since the two organic cations interact by Van der Waals forces, allowing the separation of these layers by scotch tape exfoliation in a similar way than for graphene-related materials[7,8,9]. See Figure 1.

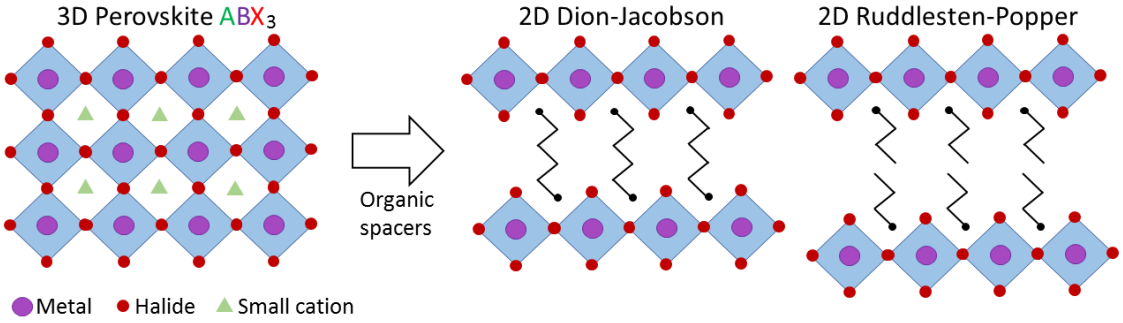

Figure 1: Crystal structure of 3D and 2D metal-halide perovskites.

Additionally, it is also possible to modulate the dimensionality of the layered metal-halide perovskites. The dimensionality refers to the number of octahedra layers sticked together, noted as n, and separated by the organic cations, see Figure 2.

1.2 Optoelectronic properties of metal-halide perovskites

Metal-halide perovskites are stand out due to their tunable optoelectronic properties by varying the composition (metal, halide, organic cation) and dimensionality (from 2D structure with n=1, 2, 3... to 3D). They have shown a high optical absorption coefficient, tunable band-gap, near-unity photoluminescence (PL) quantum yield, low trap densities and good charge carrier mobility. For example, their PL spectrum covers from the UV to NIR range. Moreover, the corresponding PL emission at room temperature ranges from extremely narrow (about 0.1 eV, thus, high color purity) to a broad width (ca. 1 eV), useful for white emitters.

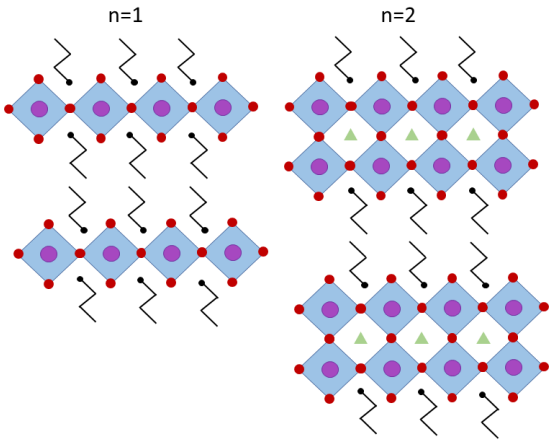

Figure 2: Different dimensionalities of the layered 2D perovskites.

The dimensionality plays an important role in the optical properties, moving from 3D to 2D structures there is a change in the valence and conduction bands dispersion which leads to larger bandgaps [10].

Not only the bandgap modulation, but there are also another advantages that the 2D perovskites offer compared to 3D counterparts. One of the main challenges is their instability under the exposure to oxygen and moisture leading to their degradation, which has been reported in the widely used lead-halide perovskites. In this sense the presence in 2D perovskite structures of large organic cations, with hydrophobic character which could act as moisture/oxygen barriers improving their ambient stability [11]. Moreover, the 2D perovskites

present a more versatile crystal structure and dimensionality than the 3D ones, which facilitates their incorporation in miniaturized and flexible electronic devices and creates new opportunities for tailor-made materials[2]. Although, the promises of the 2D perovskites seem strong, one also have to consider that the presence of the large organic cations also affect the conductivity, which is in general lower in the 2D perovskites compared to their 3D counterparts[5].

1.3 Interest and challenges

Apart from the extraordinary and tunable optoelectronic properties, the metal-halide perovskites have awakened the attention due to their low-cost processability and fabrication. These factors make them suitable for their integration in optoelectronic devices such as solar cells, light emitting devices (LEDs) and photodetectors.

However, as already commented, from the material point of view, there are several challenges in which the researchers are actively working on[2]:

- The understanding of the structure-properties-device relation to make predictable designs in terms of composition, crystal structure and target application.
- Toxicity reduction. The research work has been namely focused on Pb-based perovskites since at the moment present better performance in optoelectronic devices than other metal compositions. Lead is toxic to nature which makes devices fabrication and waste-handling in a large-scale much more complex. Nonetheless, there are many active research lines for reducing, reusing or replacing lead[12].
- Stability enhancement. Lengthening the lifetime of perovskite devices may be considered one of their main challenges. Perovskites are degraded if exposed to the atmosphere, light or temperature. The lead-halide core is easily degradable and the materials that are more stable usually come with reduced performance.

1.4 Objectives of the study

The main aims of this work are to explore and modulate the optical properties of layered (2D) metal halide perovskites for their future application in devices. For this purpose, hybrid organic-inorganic lead bromide perovskites with different organic molecules and dimensionality (n) have been used. Specific objectives are:

1. Determine the optical properties of the materials, concretely their photoluminescence emission, as bulk crystals and after their exfoliation leading to flakes, and therefore how they vary with composition, dimensionality, and thickness.
2. Enhance the environmental stability (atmosphere, light) of 2D perovskite flakes without affecting their optical properties using other 2D Van der Waals (VdW) materials such as hBN as encapsulant.

3. Rational design of heterostructures of light-emitting 2D perovskite flakes combining materials of different dimensionality, to achieve emission ranges not accessible with the starting materials and enhance the emission efficiency.

2 Experimental techniques

On this section we have described the equipment and techniques used on the experiments carried out in this work.

2.1 Exfoliation procedure

The preparation of perovskite bulk crystals follows a bottom-up methodology. The metal-halide perovskites used were synthesized by other members of the research group via a solution process in acid medium following published protocols[13]. This procedure forms macroscopic crystals of millimeter-scale (in Figure 3). From these bulk crystals, we obtained micro and nanoscale sheets (called 'flakes') via scotch tape mechanical exfoliation, see Fig. 4.

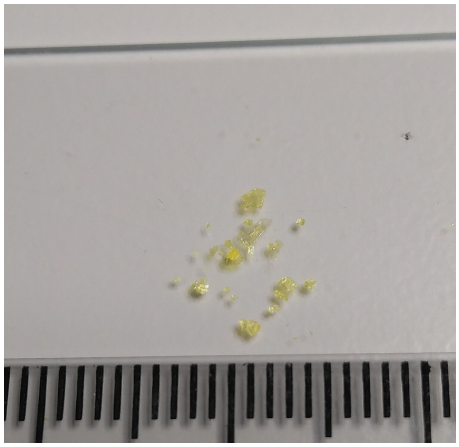

Figure 3: Millimetric-scale perovskite crystals.

The process consists on depositing a small quantity of the crystals on top of a special blue tape and exfoliate it several times until the initial small crystals are divided/sliced in small sheets. Due to the VdW nature of these materials, very thin (nm-scale) and large (μm-scale) flakes of perovskites can be obtained. To characterize these flakes, we press the tape against a polymer substrate (PDMS, Poly(dimethylsiloxane)), to physically transfer them to it.

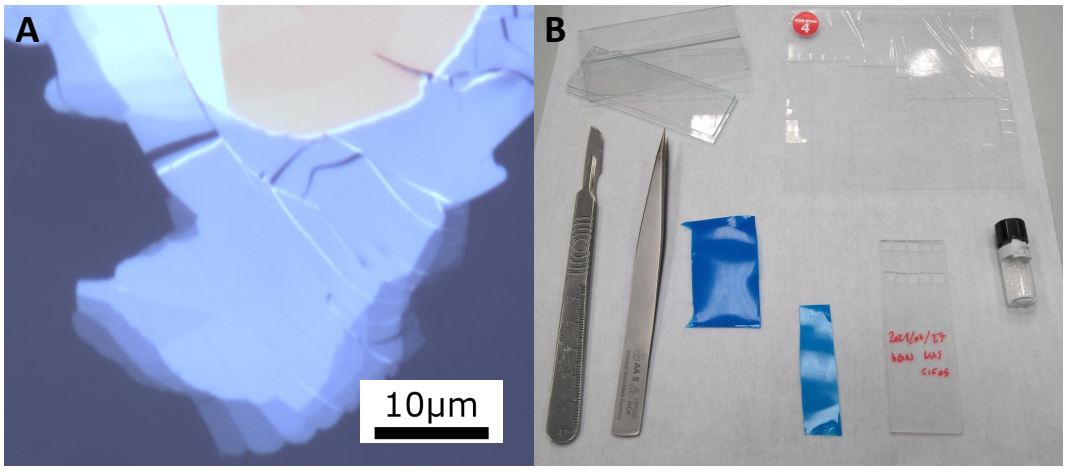

Figure 4: a) Optical microscope image of a perovskite flake. b) Laboratory tools used to exfoliate 2D VdW materials, including PDMS substrate and blue tape. The PDMS is placed on a microscope slide, to analyze the samples under the optical microscope.

Once the flakes are on PDMS, flakes with the desired characteristics are looked for using the optical microscope considering the size of the flakes. It is also used to keep record of

samples under study taking pictures to further analyse their surface features (terraces, cracks, flat sections...) or locate its position on the substrate for the corresponding experiments.

The optical microscope (Leica) used has 5x to 100x objectives, brightness/contrast customization, several light filters and a camera connected to the computer. We took photos of the flakes namely with the 50x and 100x objectives and use the software to measure their dimensions (length and width).

2.2 Dry viscoelastic stamping system

To transfer the samples from a PDMS substrate to other substrates, we have used the dry viscoelastic stamping system (a technique originally developed by Castellanos-Gomez et al[9]). The stamping system also allows to make heterostructures consisting of several flakes stacked one onto another. The substrates that are used in all the experiments are 5mmx5mm 300nm SiO_2 coated silicon, with Au/Ti markers to facilitate the localization of flakes in the next experiments (Fig. 5).

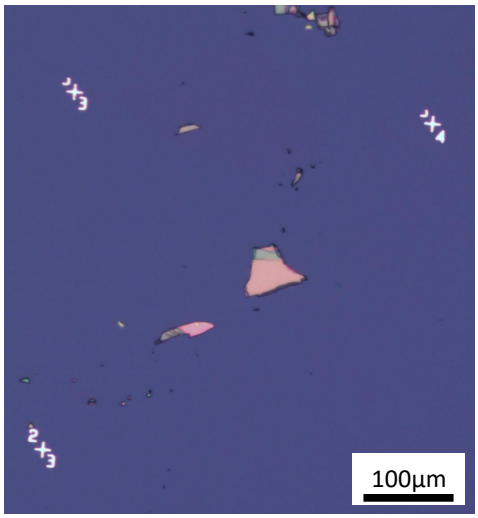

Figure 5: Perovskite flakes on a SiO_2/Si substrate with markers.

How to use the stamping system can be explained with the visual help of Figure 6. The flake that is to be transferred is on a PDMS substrate supported on a glass slide. This glass slide is mounted upside-down on a controllable arm that is moved in x,y,z-directions to reach on the SiO_2/Si substrate. This SiO_2/Si substrate is held in place by vacuum, and the holder has a 6-axis range of motion. All movement is operated manually using micromanipulators.

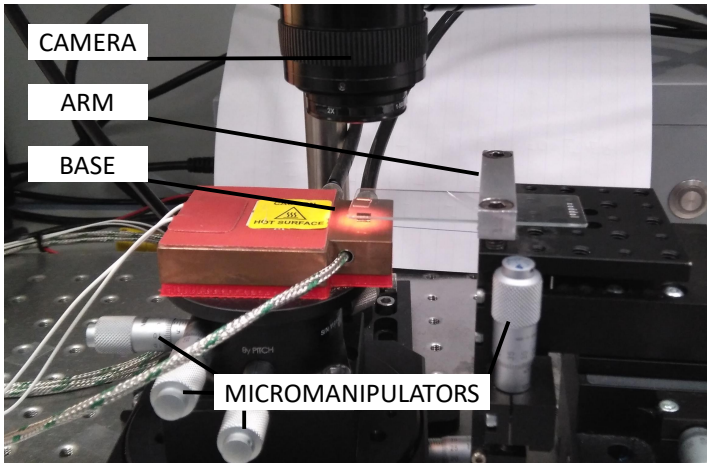

Figure 6: Image of the stamping system. Both the base and the arm are mechanically controlled by micromanipulator screws. This system is used to pass samples from PDMS substrate to SiO_2/Si.

To control both moving parts, there is a camera that gives at top down image of the setup. As both the glass slide and the PDMS are transparent, we can see the surfaces of both substrate though them and we can focus any desirable plane in the z axis. To proceed with the transfer, the PDMS is slowly lowered as we see the flake contact the SiO_2/Si substrate and then we can lift it while seeing if it is getting correctly attached or not.

2.3 Micro photoluminescence spectroscopy

The micro-Raman equipment (in Fig. 7) allows us to collect Raman and photoluminescence signal, although in this work we focused on the study of the photoluminescence (PL) emission. We used a laser as excitation source, then, the sample is excited and the light emitted is collected.

Figure 7: Micro-Raman equipment used in this work.

Therefore, photoluminescence is the emission of light from any form of matter after the absorption of photons (electromagnetic radiation) by the recombination of non-equilibrium carriers. These absorbed photons are usually provided by a light source. PL is related to the band structure of the material, and therefore, the energy of the excitation photons should be higher than the bandgap of the sample to make the process happen. Briefly and in a simple way, the absorbed photons excite the carriers from the valence band to the conduction band (low to high energy level) and the radiative relaxation of these carriers leads to photon emission (see Figure 8).

Our samples show the maximum PL emission in the 408-500nm range, depending on the compound, therefore, from the lasers available at the lab, we have chosen 405nm as excitation source. On the collection path, the light from the laser is blocked by a filter at around 405 nm, and we can collect signal from 406.5nm. To properly measure and characterize the samples, we adjusted the power of the laser and time of exposure, in order to get the best compromise between SNRR (signal to noise ratio) and avoid the damage to the sample.

The mapped area can be adjusted using the objectives ranging from 5x to 100x. We usually worked with 50x or 100x with which the laser has a footprint of $\sim 1\mu$m diameter.

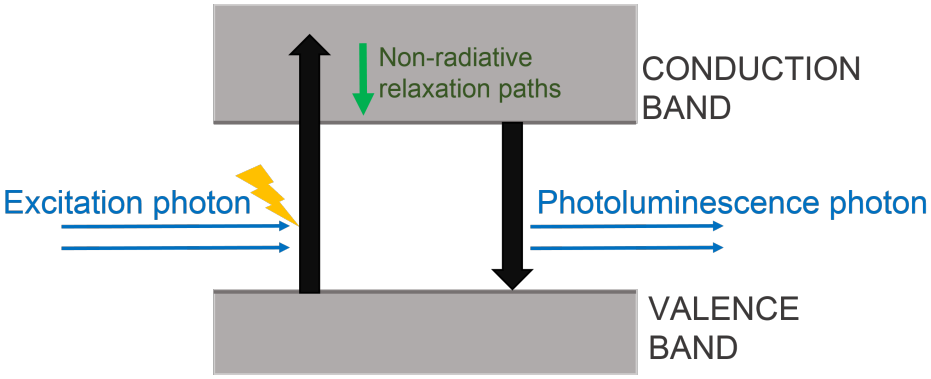

Figure 8: Scheme of the photoluminiscence process of a semiconducting material.

2.4 Atomic Force Microscopy

Thickness is an important parameter to take into account when studying flakes obtained from 2D materials. Therefore, we have used the Atomic Force Microscope (AFM) to characterize the thickness of the samples.

The AFM is a mechanical-optical instrument capable of detecting atomic forces thanks to a tip (around 200 microns long) that is attached to the end of a cantilever. When scanning a sample, atomic forces can be detected when the tip is close to the surface of the sample, which creates a small flexion of the cantilever. Thus, by measuring the movements of the reflected light of a laser pointing to the edge of the cantilever, a topography of the sample can be generated (see Fig. 9). The resolution of the AFM is below the nanometer range.

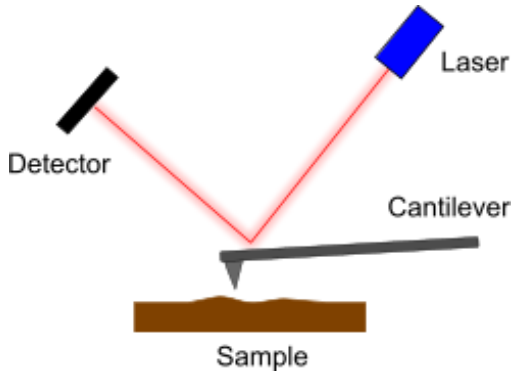

Figure 9: Scheme of the working elements of an AFM.

The experimental imaging data given by the AFM were analysed with the software *Gwyddion* to obtain the topography and thickness profiles.

3 Results and discussion

3.1 Characterization of the materials: bulk and flakes

As commented, we worked with layered lead-bromide perovskites. Therefore, in stead of the formula ABX_3, which applies to the 3D perovskites, we used the following one incorporating the presence of two cations:

$$(A')_2A_{n-1}B_nX_{3n-1}$$

where A' is the large organic cation, A is the small cation, B is the metal and X is the halide and 'n' notes the dimensionality of the crystal structure. In our case the A small cation is cesium, Cs^+; B metal is lead, Pb^{2+}; X is bromide, Br^-; and the A' is an organic cation. In this work, we used two large organic cations with different nature: phenethylammonium (PEA) with aromatic ring and butylammonium (BA) with alkyl chain (See Fig. 10).

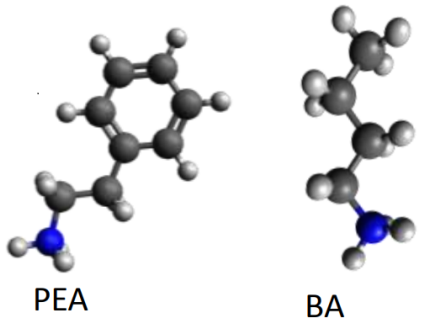

Figure 10: Scheme of the organic molecules used as the A-site cations in the studied perovskites: phenethylammonium (PEA) and butylammonium (BA).

Since in this study we aim to understand how the optical properties of the layered perovskites depends on the composition and dimensionality, we studied compounds with different dimensionality (n) or A' cation (see Table 1).

Table 1: List of the different perovskite materials to be studied in this work and the notation used along the text.

Notation	Formula
(PEA)PbBr n=1	$(PEA)_2PbBr_4$
(PEA)CsPbBr n=2	$(PEA)_2CsPb_2Br_7$
(PEA)CsPbBr n=4	$(PEA)_2Cs_3Pb_4Br_{13}$
(BA)PbBr n=1	$(BA)_2PbBr_4$

3.1.1 Absorption and photoluminescence spectra of bulk crystals

We started by measuring the absorbance and photoluminescence spectra of the bulk crystals that we exfoliate later on. To collect the spectra shown in Figure 11, we have used an UV-vis spectrometer and the micro-Raman instrument, for the absorbance and photoluminescence spectra, respectively.

Results show a systematic shift towards larger wavelengths when the dimensionality increases from n=1 to ∞ (3D) in both the absorbance and photoluminescence spectra (Table 2)

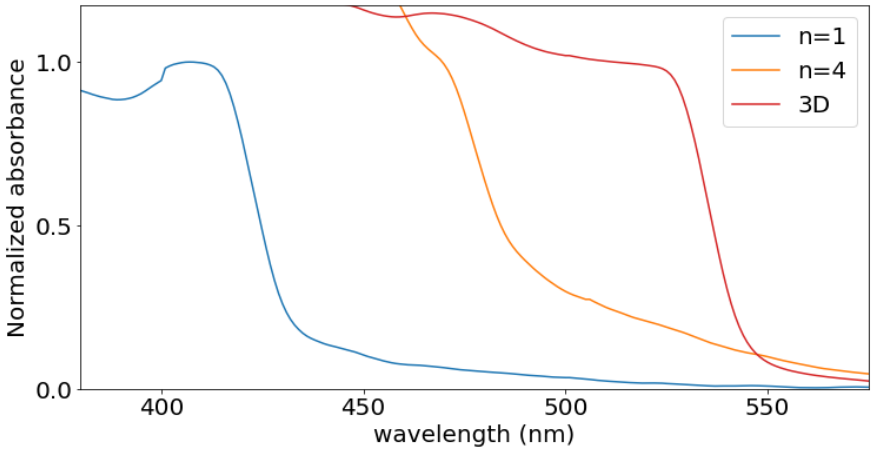

(a) Absorbance spectra.

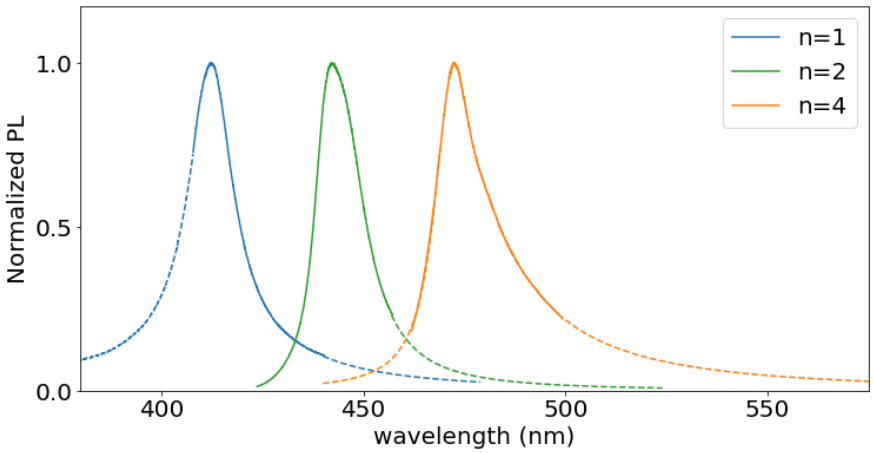

(b) Photoluminescence spectra.

Figure 11: (a) Absorbance spectra and (b) photoluminescence spectra of bulk crystals using (PEA) as organic cation of the 2D perovskite compounds of n = 1, 2 y 4, showing the shift towards larger wavelengths when the dimensionality increases from n=1 to ∞ (3D). Dashed data corresponds to fitted data.

in accordance with literature[1,5,2]. Moreover, the excitonic absorption peak is broader when comparing with the corresponding photoluminescence spectra, which is narrow. This indicates that a slight mixture of different dimensionalities is present in the crystals with n>1. The PL spectra are narrower since we analysed smaller areas of the crystals. Most important, these results demonstrate that it is possible to modulate the optical properties of these materials by tuning their composition and dimensionality.

3.1.2 Characterization of (thin) perovskite flakes

The next step of the study was the exfoliation of the bulk crystals, taking advantage of the VdW forces to obtain 2D flakes.

To facilitate the optical characterization and the building up of heterostructures with the exfoliated flakes, we first create thickness-dependent color-scale. The color-scale allow us to to quickly estimate the thickness of a flake by comparing its color with the established scale using the image taken using an optical microscope, without needing to characterize it by AFM.

As we have already seen, perovskites (and any 2D material, indeed) have colour in an optical microscope. The colour they display is related to their thickness, due to optical reasons, and creates a color palette that is always the same for each composition. In the case of perovskites it is very colorful. The goal is to inspect and photograph these perovskite flakes while they are in a PDMS substrate, then stamp then to a SiO_2/Si substrate to characterize them by AFM. Ultimately, both sets of data, optical image and AFM topography, can be put together to get a scale bar that relates the colour with thickness.

Sample preparation: exfoliation and stamping

For this purpose, flakes of each perovskite compound studied have been selected. To make the comparison easier, we selected flakes with terraces, ranging from very thin (10 nm) up to ∼100nm, where it cannot be considered as a 2D material anymore. Pictures of these flakes have been taken by fixing the same settings in the optical microscope (brightness, contrast, white balance, objective, exposure time...).

The selected flakes are then stamped onto a SiO_2/Si substrate. After it, some more pictures have been taken to later localized the flakes under the AFM instrument. It has to be noted out that the contrast of the colours of the samples change on the SiO_2/Si substrate, making more visible the thinnest flakes. However, for the colour-scale elaboration, we only use optical imaging onto PDMS substrates, since we use the PDMS substrates to select the samples.

AFM characterization: colour scales

Every sample is mapped by AFM imaging, obtaining thickness profiles and topography images. This has been successfully done for the four perovskite compounds. The corresponding thickness profiles (and all the intermediary data) are shown in Figure 12. Analysing the colour-scales obtained for the different materials, we observe that:

Table 2: Optical properties of the bulk crystals studied.

Compound	Dimensionality	Absorbance peak (nm)	PL peak (nm)
$(PEA)_2PbBr_4$	n=1	410 ± 1	408 ± 1
$(PEA)_2CsPb_2Br_7$	n=2	446 ± 1	444 ± 1
$(PEA)_2Cs_3Pb_4Br_{13}$	n=4	470 ± 1	472 ± 1

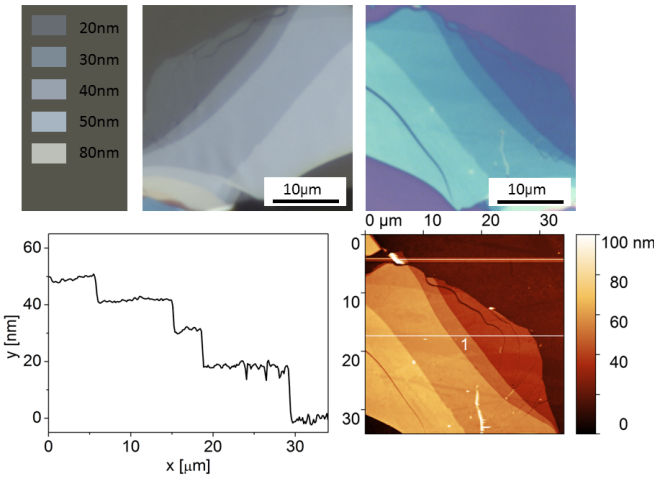

(a) Perovskite structure: (PEA)PbBr n=1

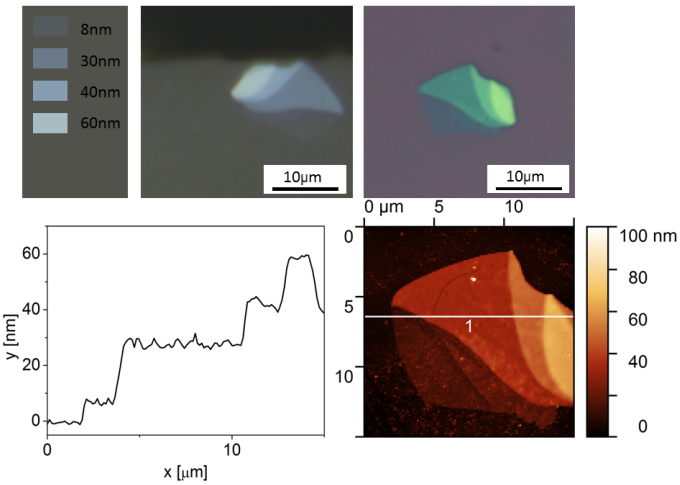

(b) Perovskite structure: (BA)PbBr n=1

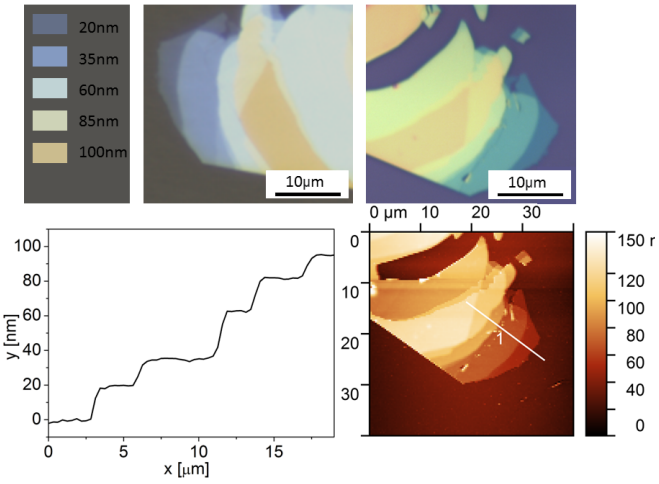

(c) Perovskite structure: (PEA)CsPbBr n=2

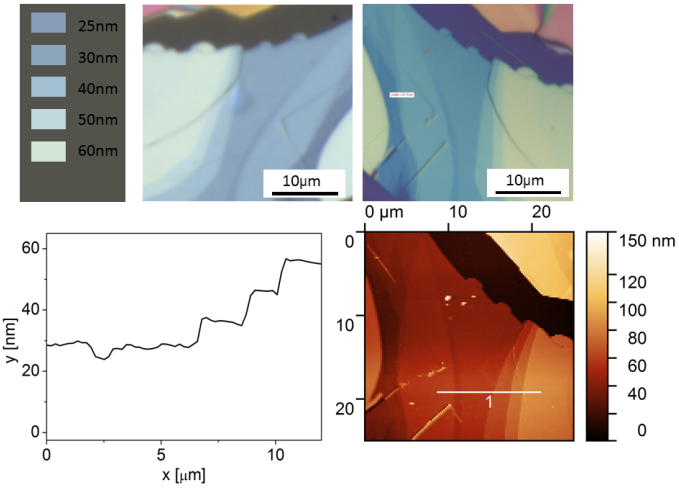

(d) Perovskite structure: (PEA)CsPbBr n=4

Figure 12: Study of the thickness of the four perovskite compounds used in this study. For each structure, there is an image of the flake in PDMS, an image of the flake in SiO_2/Si substrate; both via optical microscope. On the bottom row of each picture it is displayed the AFM topography image of the flake on the right, and the corresponding height profile (from the white line on top of the AFM image) on the left. The color-thickness palette is displayed on a background of matching colours with the PDMS.

1. When moving from bright colors (orange, yellow) to grey shades, the thickness decreases. All samples are greyish below 60nm.

2. Different perovskite compositions have different palettes.

   (a) A higher dimensionality n brings a brighter colour.

   (b) The organic component has a smaller impact, both n=1 compounds are very similar.

3. There is an exfoliation limit: flakes of below 20nm are difficult to obtain. This study aimed for thin samples and yet only the (BA)PbBr had bellow 20nm thickness[1].

These remarks offer useful information for sample preparation and experiment design in the upcoming sections of this work.

Effect of flake thickness on the photoluminescence properties

As done for the AFM thickness determination, we prepare flakes with terraces to evaluate the effect of the flake thickness on the PL properties in terms of peak intensity, position and line width (FWHM). The aim is also to determine the experimental detection limit of PL considering the flake thickness.

We have focused our efforts on n=1 and n=4 structures, which are used to create perovskite heterostructures further down in this work and for which this thickness study is intended. The change in intensity of the PL of the flakes can be seen in Figure 13.

For the n=1 perovskites, both phenethylammonium (PEA) and butylammonium (BA) compounds have been studied and both show a systematic increase of PL intensity with the thickness. This increase has a linear nature in every perovskite type, as the curve fitting done have small errors. It is important to note that there was no detectable PL intensity for thickness $< 10nm$. Therefore, we work for the next steps with flakes of thickness $> 20nm$. Moreover, some degradation was observed for the (BA)PbBr n=1 samples, but it is futher discussed in the stability experiments.

By analising also their respective peak position and full width half maximum (FWHM) dependence with the thickness (Figure 13), we observe that: (i) both peak position and width systematically increase with thickness, (ii) the increase in the peak position is small and not significant considering the instrument error $\pm 1nm$.

[1] This composite, (BA), gives much thinner samples while exfoliating.

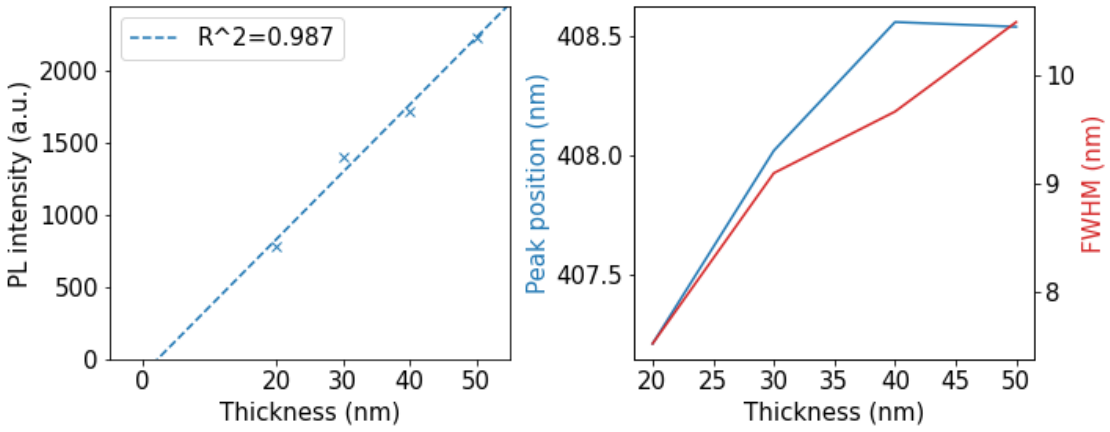

(a) Perovskite compound: (PEA)PbBr n=1

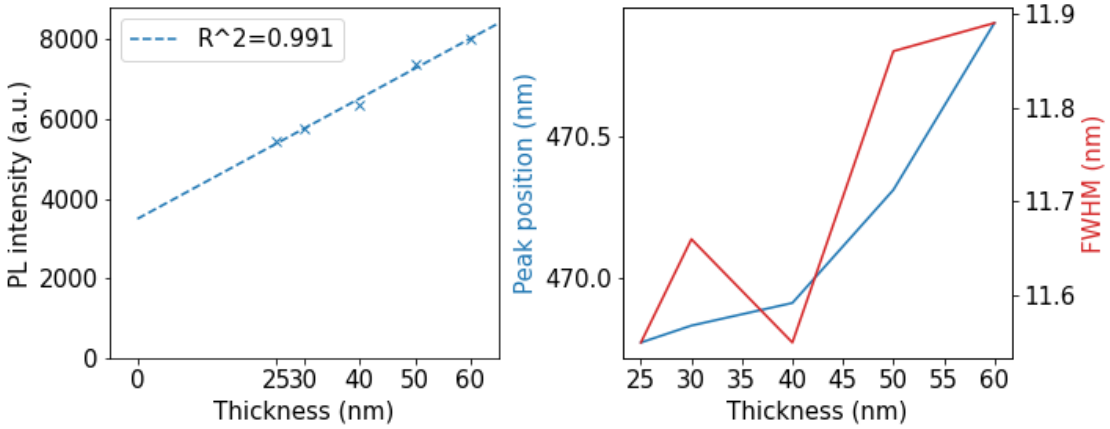

(b) Perovskite compound: (PEA)CsPbBr n=4

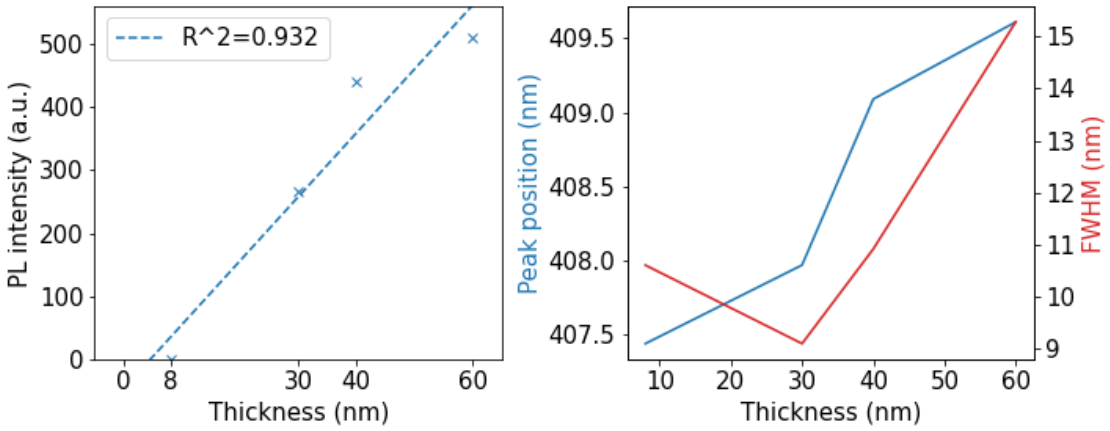

(c) Perovskite compound: (BA)PbBr n=1

Figure 13: Photoluminescence emission characterization of the perovskite compounds. Left, the intensity as a function of thickness is displayed and, on the right, the respecting peak position and FWHM. A linear curve fit has been performed on the intensity graphs.

3.2 Stability study

3.2.1 Exposure to the atmosphere

Perovskite stability is one of the main disadvantages of these materials, since they are affected by different factors, primarily the atmosphere, but also light and heat. On this study, we aim to evaluate the degradation effect of the atmosphere depending on the organic cation and the dimensionality of the perovskite. Regarding to the atmosphere, it has been described in literature that the main sources promoting the degradation are oxygen and moisture, especially the latter one. It is not correct to describe this process as a simple oxidation, as it is rather a mixture of multiple redox reactions that form oxides and hydroxides[4].

Looking at the literature, we can gain information on the degradation paths and the conditions in which they can happen. Regarding to the widely used and studied $MAPbI_3$ 3D structure[2], the group of Ruoting Dong[4] analysed its degradation against moisture proposing a reversible first reaction (1), then followed by (2), an irreversible loss of MA. An excess of water therefore moves the equilibrium (1) towards the formation of products.

$$4\,[(CH_3NH_3)PbI_3 \cdot H_2O] \;\Leftrightarrow\; (CH_3NH_3)_4PbI_6 \cdot 2H_2 + 3PbI_2 + 2H_2O \quad (1)$$

$$(CH_3NH_3)_4PbI_6 \cdot 2H_2 \;\Leftrightarrow\; 4CH_3NH_3I + PbI_2 + 2H_2O \quad (2)$$

We expect a similar principle for the reactions in our Pb-Br samples. There may be other ways of degradation that the mentioned one, but the moisture and oxygen are always be strongly implied. For that, this work does not focus on the nature of the degradation, but rather on the effectiveness of the ways used to prevent it. As a reminder, the strategies already used in the samples studied that help to minimize the degradation are the following:

1. The use of bromide instead of iodine. Perovskites of Pb-I have been widely studied and proposed for high performance optoelectronic devices, but the exchange of Br makes the perovskites more stable[14].

2. Layered 2D perovskite structures have a better moisture tolerance due to the hydrophobic nature of the organic molecules used in the A'-site[11].

With these changes, the samples studied in this work are much more resistant and it helps to their study and characterization in the laboratory, but mean no long-term solution for their stability issue. Looking for a long-term protection, here we propose the encapsulation of 2D thin perovskite flakes with hBN flakes and compare their behaviour under ambient exposure with unencapsulated flakes.

As commented, the material proposed for the encapsulation is crystalline h-BN (hexagonal boron nitride). It is an atomically thin layer of a graphene-like hexagonal structure

[2]MA stands for the methylammonium cation, CH_3NH_3+.

of alternating boron and nitrogen atoms[15]. These layers are held together by Van der Waals (VdW) forces, and are spaced every 3.3$\mathring{A}$[15]. Therefore, their mechanical exfoliation is possible.

In relation to its optoelectronic properties, hBN is an insulating material with a wide bandgap, of around 6eV. It has been reported in literature that bulk hBN has an indirect bandgap of 5.95eV and a monolayer has a direct bandgap of 6.1eV[16,17]. It is considered a transparent material as it has a very low absorption in the 250-900nm range, but with a strong absorbance peak around its bandgap (i.e. 200-220nm)[15].

Therefore, this material is a good candidate to encapsulate the perovskite samples since: (i) It has optical transparency in the wavelength range of interest for the study of the perovskites photoluminescence; (ii) It is an insulating material, limiting charge transfer process through the barrier; and (iii) It is non-permeable and has already been reported to block moisture and oxygen gas acting as a gas barrier[18].

In order to carry out the ambient exposure study, the perovskites were stored in darkness and room temperature conditions.. Regarding to humidity, we monitored it and it has maintained a value between 55% and 65% RH (Relative Humidity) throughout the study. This value is higher than 30%, usually considered as dry conditions for perovskites. Thus, the oxygen and moisture in the atmosphere should be the main degrading factors.

Since the PL emission of the hybrid organic-inorganic metal halide perovskites is sensible to any mode of degradation, we monitor the PL spectrum of the different materials under study to evaluate the effect of the exposure to the atmosphere in terms of:

1. Intensity: Rough estimation of thickness. It also gives the general performance level of the perovskite and its weakening is an indication of degradation.

2. Peak position: there are more factors affecting the position of the PL peak. Slight variations in the range of a few nanometers can be due to: thickness[3] or strain, for instance. But usually, a shift towards shorter wavelengths can be a signal of degradation.

3. FWHM (Full Width at Half Maximum): As shown in Figure 11b, the materials present a narrow linewidth. Therefore, a broadening of the PL spectrum or the appearance of shoulders have been attributed to indications of degradation or surface defects.

In this experiment we tracked several perovskite samples, and measured their PL spectra as they are exposed to the laboratory's atmosphere during several weeks. To understand the effect of the use of a hBN flake to encapsulate the perovskites, both flakes with and without covering are studied. Regarding to sample preparation, hBN is commercially available as powder crystals that we mechanically exfoliated with the blue tape to obtain thin[4] layers. These layers are transferred on top of the perovskite samples with the dry-viscoelastic stamping system described in the experimental chapter. We have used single-side encapsulating

[3]The relation between thickness and PL of $(C_4H_9NH_3)_2PbBr_4$ has been reported by Letian Dou et al[19], where a smaller thickness is related to a bigger band gap.

[4]Not monolayers, as their obtainment and detection with the used methods has not been possible.

(i.e. Si/SiO_2-perovskite-hBN stacks) where hBN is on top of the perovskite flake and completely surrounds it by being in contact with the SiO_2/Si substrate all around 360 degrees of the flake (see Fig. 14).

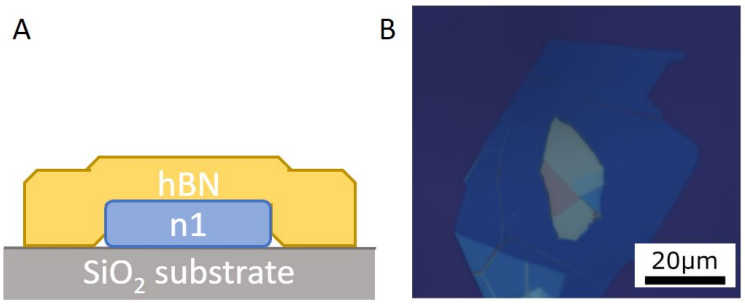

Figure 14: Encapsulation of a perovskite flake under an hBN flake. a) Scheme, b) optical microscope photo.

To make accurate measurements, tracked samples have a main flat section, so that the expected degradation happens uniformly and PL can be consistently collected using several points for each sample. To faccilitate the data analysis, an average of 5 measures of PL are taken (equidistant points on a straight line, for the sake of simplicity and reproducibility). Each sample is studied every week for 1-2 months. A *Python* code is used to analyze all the spectra. Each point gets parameterized by a Gaussian, which gives the following parameters: height, peak position and linewidth. These parameters get averaged. The mean value $\hat{x}$ and mean square error Δx of an N-long sample of data $\{x_i\}_N$ are obtained via the next formulas:

$$\hat{x} = \frac{1}{N}\sum_i x_i \quad ; \qquad \Delta x = \frac{1}{N(N-1)}\sqrt{\sum_i (x_i - \hat{x})^2} \tag{3}$$

The results of these measurements after (at least) three weeks of data collection (depending on the sample), are displayed in Figure 15. As can be seen, we have obtained the degradation trend for the different samples. All the samples corresponding to the same compound are grouped together in the graphs.

Evaluating the results obtained, we observe that:

1. The PL intensity decay of the perovskites occurs in two steps. First, there is a quick decrease of the PL intensity in the first 1-2 weeks, that seems to affect the layers closest to the surface. Then the decrease is slower. A possible explanation is the formation of a passivation layer. The flake degrades from the surface to the substrate. Therefore, the first superficial layers degrade leading to a degraded layer that protects the underneath layersfrom moisture acting like a barrier. From the trend of the PL intensity curves in the uncovered perovskite graphs, this passivation layer should be formed within the first 1-2 weeks. Then the PL intensity stays almost constant. Depending on the flakes thickness, the relative proportion of the passivation layer is different, explaining why we still observe PL emission on the thicker samples vs. the thinnest ones.

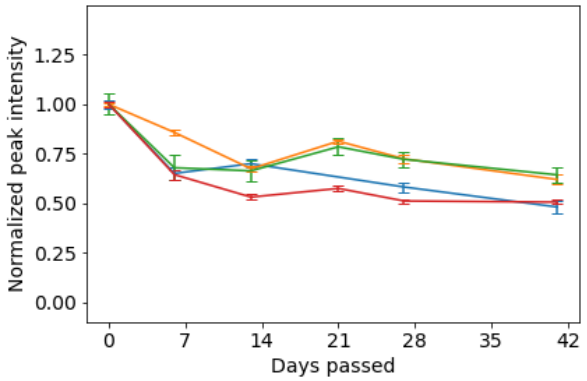

(a) Structure: (PEA)PbBr n=1

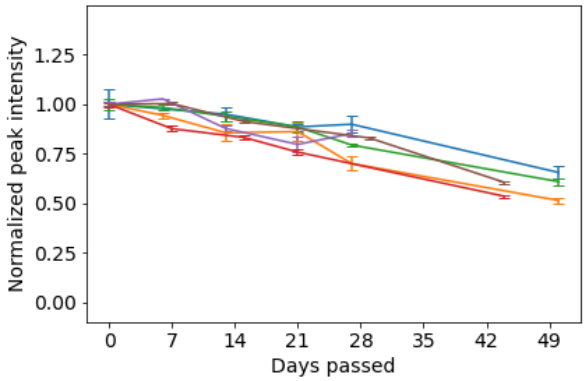

(b) Structure: (PEA)PbBr n=1 w/ hBN

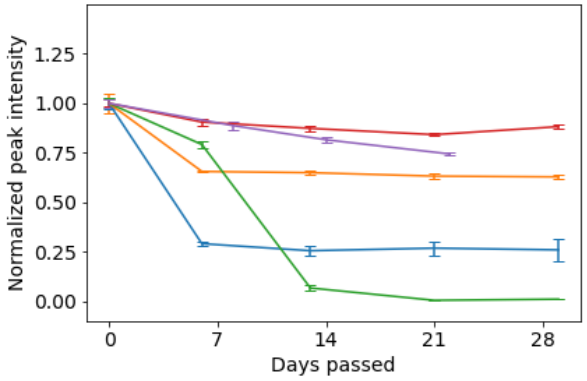

(c) Structure: (PEA)CsPbBr n=2

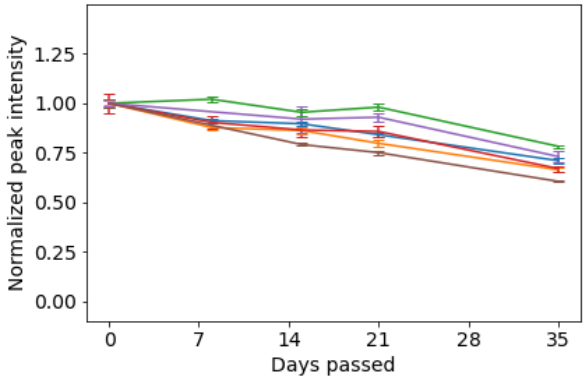

(d) Structure: (PEA)CsPbBr n=2 w/ hBN

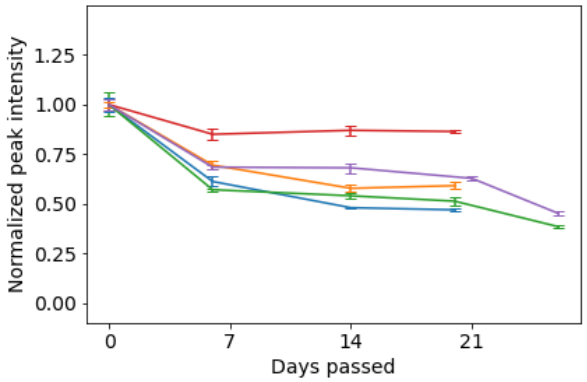

(e) Structure: (PEA)CsPbBr n=4

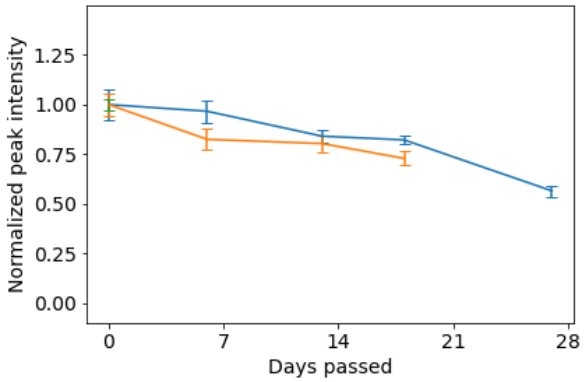

(f) Structure: (PEA)CsPbBr n=4 w/ hBN

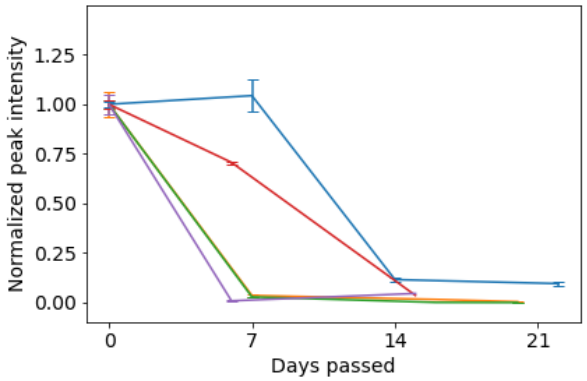

(g) Structure: (BA)PbBr n=1

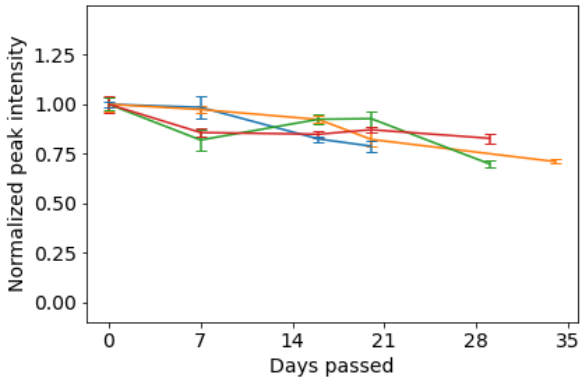

(h) Structure: (BA)PbBr n=1 w/ hBN

Figure 15: Study of the atmosphere stability of different perovskites. Evolution of the PL intensity of the studied samples, catalogued from a) to h) by composition.

2. If we compare the effect of the organic cation: phenethylammonium (PEA) and butylammonium (BA) on the stability: First, we can clearly see that (BA) samples are much more unstable and therefore the PL intensity decreases in the first days of exposure, being more marked for thinner flakes (see Fig. 16). This highlights that the PEA cation offers a better ambient stability.

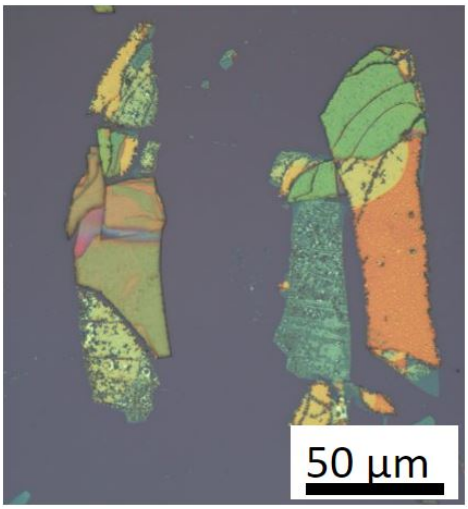

Figure 16: Optical microscope image showing the strong degradation observed on a (BA)PbBr n=1 sample after 15 days of atmosphere exposure.

3. Regarding to the dimensionality n, there are no big differences between the different (PEA) compounds when comparing their stability. Therefore, the organic cation is playing the main role in the stability, while the dimensionality is most important for the modulation of the optical properties.

4. Lastly, we have the effect of hBN encapsulation. The degradation speed is slowed, and the PL intensity drops ever so slightly over the weeks. The protection is not completely perfect and the samples are degraded over time, maybe due to reported leaking moisture and oxygen through hBN defects[18]. Nevertheless, after a month of exposure the samples retain ∼80% of their initial intensity, acting as efficient encapsulation. More over, the samples of (BA) covered by hBN have an outstanding stability and show similar decay rate of the (PEA) compounds, even though they are more unstable. Therefore, we demonstrate that hBN protects independently of the perovskite composition.

As a conclusion, hBN single-side encapsulation succeeds in making a simple, efficient solution to perovskite degradation, and keeps the PL intensity over 70-80% after 3 weeks for all the samples, which was the target duration suited for research purposes in the laboratory. It gives good protection to unstable varieties of perovskites, allowing the research of the unstable (BA)PbBr, or even (PEA)PbI, outside of inert atmospheres such as argon or nitrogen commonly used for keeping or characterizing devices at the lab-scale.

3.2.2 Exposure to light

Not only to the atmosphere but metal-halide perovskites are sensible to other external stimuli as light, which is the one primarily reported. Indeed, while conducting the moisture stability study, some insight of the degradation of the perovskite samples to light was observed. We noticed that room-light or optical microscope light enhances the degradation of perovskite samples, mostly seen in the more sensitive (BA) samples. A good understanding on the degradation with different external agents is of great value to fully understand how perovskites behave.

Akihiro Kojima et al[20] studied the light-induced decomposition of 3D perovskites. They show the difference between the use of iodine and bromide, as the latter is used specifically for its longer stability. The decomposition of both varieties, $MAPbI_3$ and $MAPbBr_3$, was studied and the degradation paths are detailed in (4) and (5).

$$MAPbI_3(s) \xleftrightarrow{h\nu} PbI_2(s) + Pb^0(s) + I_2(g) + CH_3NH_2(g) + CH_3I(g) + HI(g) + NH_3(g) \quad (4)$$

$$MAPbBr_3(s) \xleftrightarrow{h\nu} PbBr_2(s) + CH_3NH_2(g) + HBr(g) \quad (5)$$

They show that the creation of $CH_3NH_2(g) + HX$ (where X is I or Br) is considered a reversible degradation as they actually are the precursors for the synthesis of the perovskite. These products can be lost, if the gases leak from the perovskite, thus making the reverse reaction not possible. An encapsulation of the flakes for preventing the volatile precursors leaving the surroundings of the generated $PbBr_2$ may benefit a possible regeneration of the perovskite structure.

Moreover, we can see the differences between the decomposition of iodine or bromide. The former also generates products of thermodynamically less favourable reverse reactions. Therefore, bromide perovskites offer clear and favourable regeneration, being a better choice.

To conduct this study, we used an analogous procedure as in the previous atmosphere stability study. Again, we carried out PL measurements to monitor the samples before and after the light exposure.

As for the samples, they are thin (< 500nm), to get the light absorbed through all the depth of the flake, and flat, to be able to get a consistent measure of their PL emission. Samples were also covered in hBN to discard additional effects of the atmosphere. Some control samples without hBN coating act as control samples, to understand the effect of hBN on the process. As for the light source, we used a white LED light, with a broad spectrum displayed in Figure 17. To carry out the light exposure, we used a dark box with the light placed on the top cover and a power density of $64.3 mW/cm^2$ (during all the measures).

In a systematic way, we exposed the samples to the light source on timed, increasingly longer periods and we measure their PL emission after each period. After this light exposure period, the samples are left to recover and reach an equilibrium state, and further PL measurements are carried out.

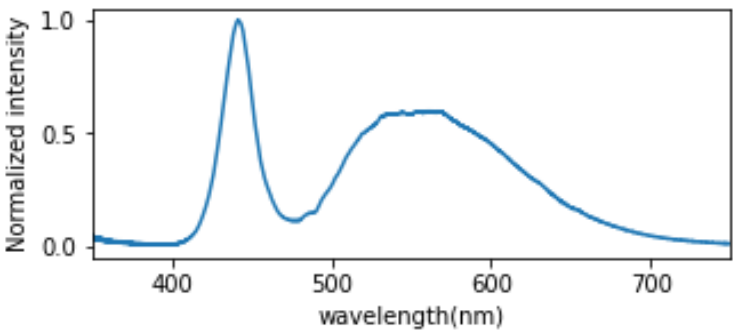

Figure 17: Emission spectrum from the white light source used in the experiments of section 3.2.2.

Effects of hBN encapsulation

We measured (PEA)CsPbBr n=4 samples, on several hBN-covered and uncovered flakes. The samples are excited simultaneously on intervals which sum up to 1 hour. After that more measurements have been taken after certain rest time, to see what the reached stable state is. This experiment gives general understanding of the effects of the light exposure. We also evaluate the effect of hBN coating and compare results with uncovered samples.

For the sake of a better visual understanding, representative example of those samples are shown in Figures 18 and 19. The key points that can be extracted from the experiment can be synthesized in the following points:

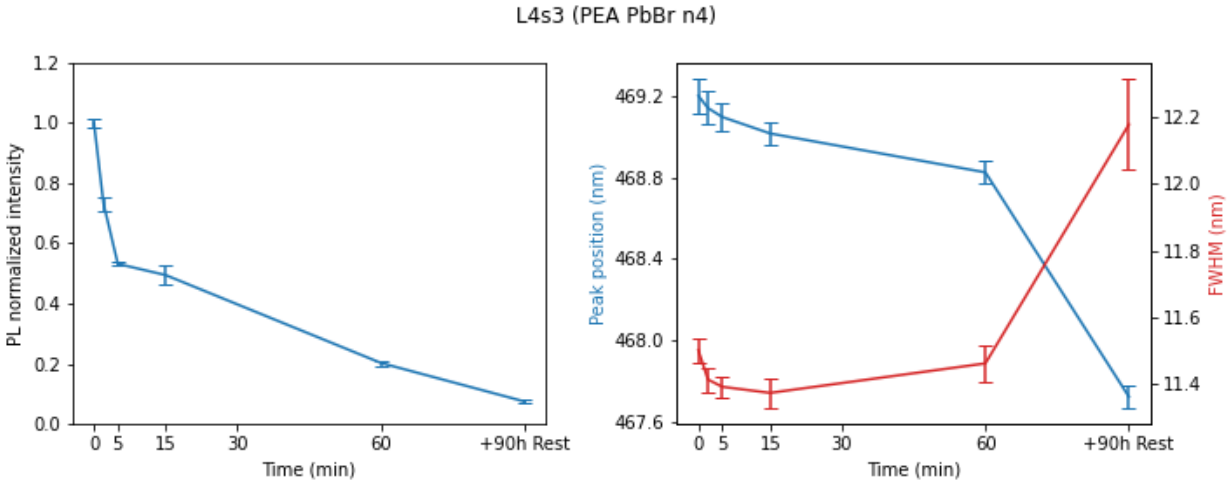

Figure 18: Results extracted from the photoluminescence of a representative uncovered n=4 sample, during the light exposure study. (Left) Value and error on the average intensity of the PL. (Right) Idem for the peak position and FWHM.

- Effect in uncovered flakes:
  - The PL intensity decreases when increasing the exposure time, reaching the 40% of their original value by 1h. The decrease is not constant, and most of the damage/degradation happens in the first 15 min and an equilibrium is reached afterwards.
  - Changes to peak position or FWHM were not significant, although a systematic blue-shift[5] and broadening is observed confirming degradation pointed out by the clear PL intensity decrease.
  - After a day of rest, the peak position and the FWHM changed substantially. Those changes were slow, as little change happened after 30 min, compared to a full day of rest.

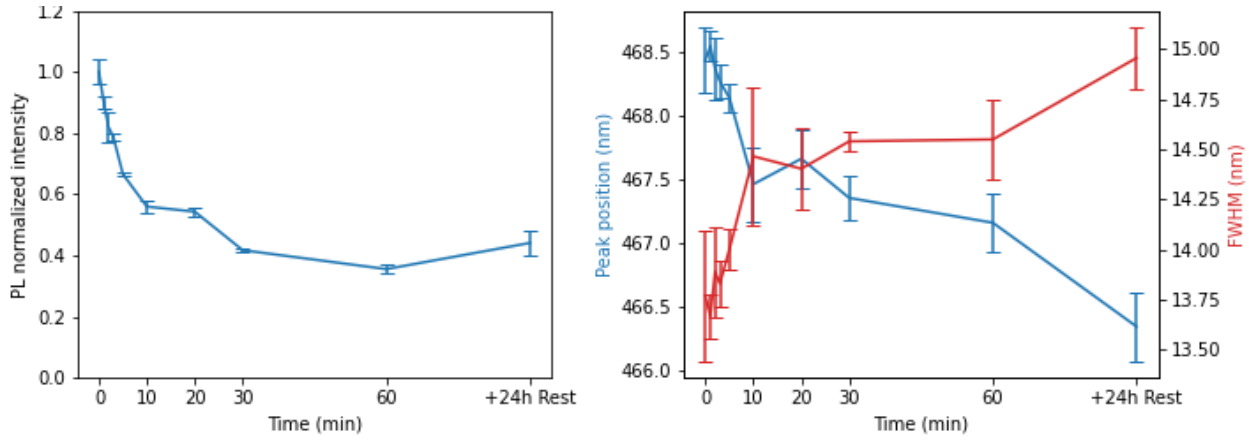

Figure 19: Results extracted from the photoluminescence of a representative hBN covered n=4 sample, during the light exposure study. (Left) Value and error on the average intensity of the PL. (Right) Idem for the peak position and FWHM.

- Effect in covered flakes:
  - These samples were also damaged by the light exposure. They had a decrease of the same order in their intensity. It shows that light goes through the hBN layer. Those changes happen happen after the exposure time, similar to the uncovered case.
  - There have been more significant changes in peak position and FWHM during the light exposure period.

To sum up, hBN does not reduce the light-induced degradation, as light goes through it. Most important, the encapsulated samples showed more significant changes in the PL spectrum (position and linewidth), which maybe indicate that degradation products formed remain inside and continue to damage the flake.

[5] An enlargement of the bandgap is called *blue-shift* as the resulting PL of the material moves towards a blue color.

Effect of the dimensionality: n=1 & n=4

We also evaluated the light exposure on (PEA)PbBr n=1 perovskite and compared with the n=4 results using hBN for encapsulation. The different absorbance spectrum of both materials could play a role, since the overlap with the white LED spectrum is smaller in the case of the (PEA)PbBr n=1. Nevertheless, this does not mean that the light cannot induce any degradation on the material.

As the monitoring of the PL intensity shows, Figure 20, we observed a similar behaviour than in the n=4 perovskite. The behaviour is reproducible in the 3 samples of (PEA)PbBr n=1 studied.

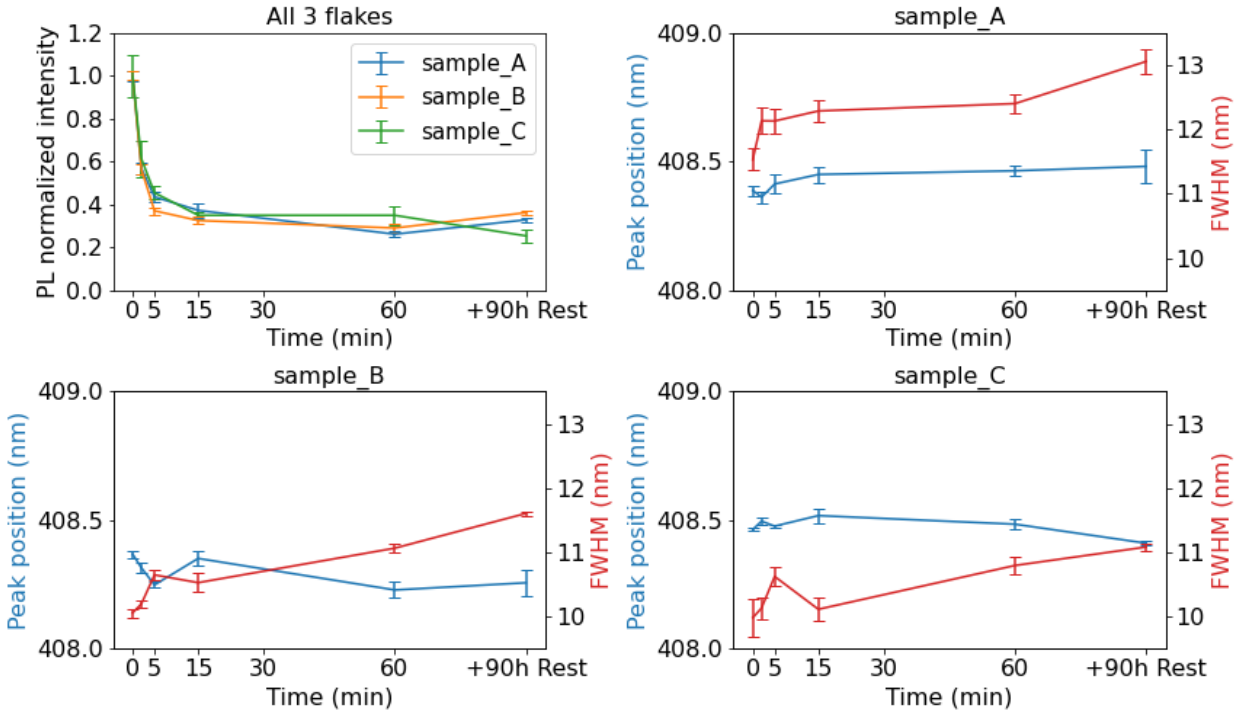

Figure 20: Evolution of the phololuminescence intensity of representative (PEA)PbBr n=1 samples, covered by hBN, through exposure to a white light source. The PL intensities of the 3 samples are displayed in the top left graph. The corresponding peak position and FWHM of each sample are shown in separate graphs.

As happened with the encapsulated (PEA)CsPbBr n=4, in the (PEA)PbBr n=1, results pointed out that:

- The PL intensity exponentially decreases from the initial value to roughly 30%-40%. The relative decreases from Fig. 20 and the already displayed Fig. 18 are similar in trend and magnitude. The only variation of the total loss depends on the thickness of the samples, as thin ones have shown more decrease, while thick ones have lost less than 60% of their PL intensity.

Lastly, it also is clear that no changes in intensity appear after the exposure time is finished. With these results, we demonstrate that independently of the light absorbed the light degradation occurs.

- Regarding to the FWHM, it always broadens. The increase is bigger in the first stages of the exposure, where the PL intensity drops the most. It also broadens substantially after the exposure period. Not only in the samples shown in Fig. 20 (in red) , but every other sample has a consistent line width broadening.

  The evolution of FWHM is similar between n=1 and n=4 samples, and the broadening observed supports the degradation highlighted by the PL intensity decrease.

- Looking at the peak position of the three n=1 samples in Fig. 20 (in blue), the change in position lies within the order 0.1nm, much smaller that the change reported on n=4 samples, which was of a few nanometers. Considering the experiments performed, we have seen that uncovered-hBN perovskite samples have consistent small blue-shifts, while covered flakes usually display none. When a hBN-covered sample has this blue-shift, it is thicker. Therefore, the main factor that seems to be the thickness since only the thinnest samples present the peak position blue-shift, indicative of degradation.

Therefore, we can conclude that white light exposure affects the two different perovskite n=1 and n=4 in a similar way. Therefore, there are no big changes on their behaviour under light exposure.

Effect of thickness

Additionally, we have studied the effect of thickness on the photodegradation. Making use of the colour-scale obtained in section 3.1.2, we have reevaluated the analysed samples, as can be seen in Figure 21.

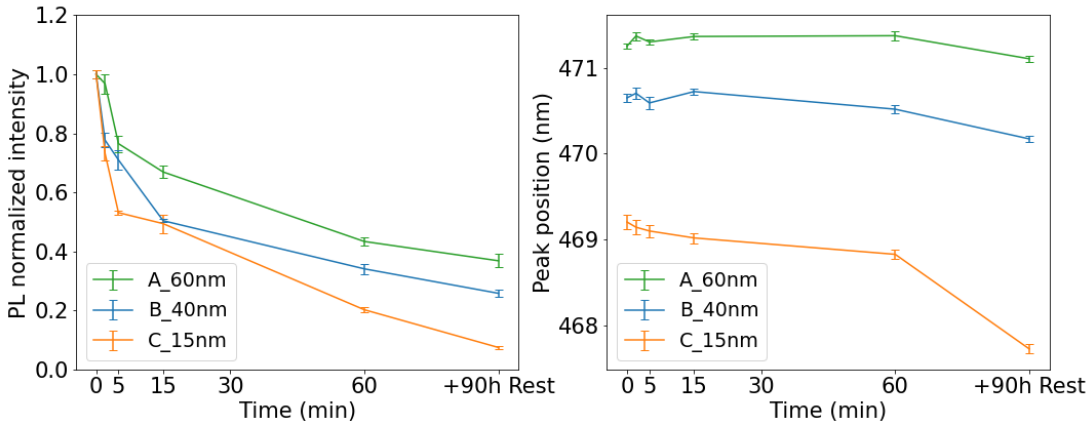

Figure 21: Phololuminescence emission of uncovered (PEA)CsPbBr n=4 samples, under exposure to a white light source. The intensity of the photoluminescence is displayed in the left graph, while the peak positions are displayed together in the right graph.

The drop of the PL intensity is proportional to the thickness of the sample: thin samples lose a larger part of their PL intensity, while thicker need more time to show the degradation.

As for the FWHM, there is not a clear relation with the thickness but all the samples get a wider spectra after the light exposure, independently of their thickness, indicating the degradation. This broaden of the PL peak is also accompanied by a blue-shift of the peak position, being larger for thinner samples. Therefore, corroborating the degradation with the light exposure.

3.3 Building heterostructures

The aim of this section is to modulate the resulting photoluminescence emission of the individual flakes by creating heterostructures to enhance the efficiency of one compound or even create a sum of colours. For this purpose, we made vertical stacks combining perovskites with different dimensionality. Concretely, considering the previous experiments on PL characterization, exfoliation and stability, we selected (PEA)PbBr with n=1 (PL emission at ca. 408 nm) and n=4 (PL emission at ca. 470 nm). When putting in direct contact the flakes, their Van der Waals nature and band energy levels alignment allow the energy transfer between them. The direction of the energy transfer goes from the larger bandgap (n=1) to the shorter bandgap (n=4) material, as a type-I band alignment [21]. Some transfer examples can be studied in Figure 22.

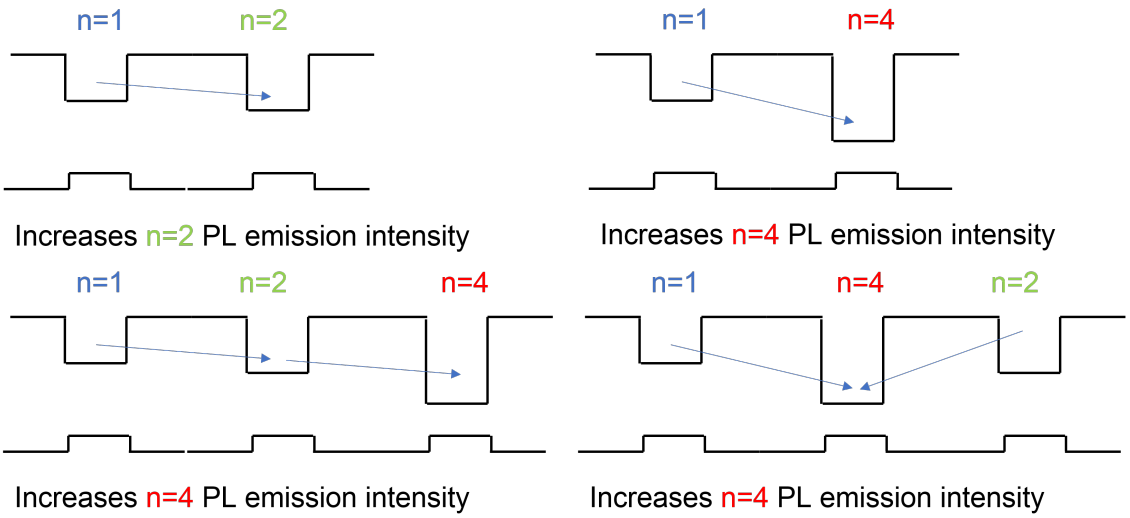

Figure 22: Expected transfers between different heterostructure combinations, all of type-I band alignment. The two lines of every scheme indicate the conduction band (top) and valence band (bottom) structure along the heterojunction.

Therefore, for the building of the heterostructures, we evaluated the following parameters: (i) combination of the materials, (ii) the presence of an isolating and transparent material (hBN) and (iii) the thickness variation of the flakes. For the experimental design, we assembled all the heterostructures using the PDMS stamping technique leaving parts of the flakes out of the structure and characterized them by micro-PL spectroscopy. We used the parts of the flakes out of the structure as control to observe the PL emission of each material and compare with the heterostructure.

3.3.1 Effect of the order of the stack

As commented, the first point to consider is the order of the materials in the vertical stack: n1/n4 or n4/n1. Regarding to notation, the layers are named from bottom to top. For instance, a n1/n4 heterostructure would be n4 flake on top of n1 flake.

Order of the heterostructure: n1/n4

We started with a n4 flake on top of a n1 one, using flakes thickness <200nm to allow the excitation to arrive the bottom flake. This should give an enhanced n4 emission, which we target. As commented all the heterostructures on this section have been assembled with the stamping system. It was important to stack the flakes so that we leave parts of those flakes out of the structure. Therefore, we can measure the signal of the heterostructure and compare it to the original signal of the flake (See graphic explanation in Fig. 23).

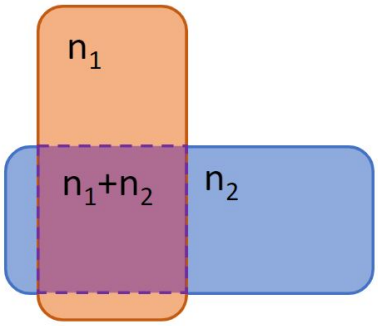

Figure 23: Top view of what the heterostructure organization should be.

A representative sample, and its photoluminescence emission, is shown in Figure 24. We observe that the PL intensity of the higher-n compound is clearly enhanced, by the portion of lower-n PL emission that is transferred to it, in accordance with results in literature done with other perovskites[21]. Concretely, the PL emission intensity of n4 is enhanced by a factor of 2, while the n1 one is reduced to half of the initial one. This behaviour is of high interest and worth to be studied.

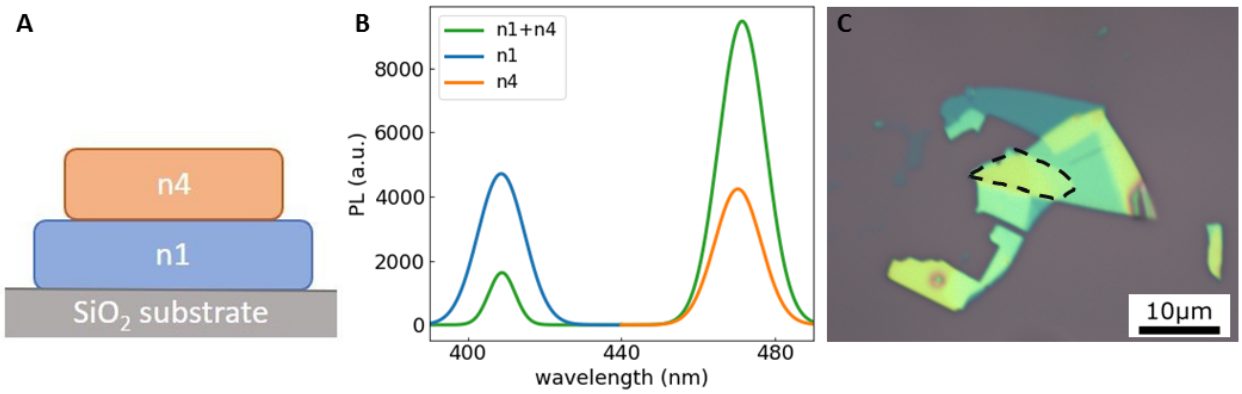

Figure 24: Analysis of a representative n1/n4 flakes heterostructure. (a) Order of the heterostructure. (b) PL emission of the heterostructure, in green, as well as the original emissions from n1 and n4. (c) Optical image, with the heterostructure in the highlighted area.

Order of the heterostructure: n4/n1 (n1 on top of n4)

Now we have inverted the order of the components. In principle, this should affect the result. In this case, part the excitation light is already absorbed by n1, thus, the power excitation reaching the n4 flake is lower than in the previous stack n1/n4. Moreover, n4 PL emission can pass without being absorbed by n1 flake if one consider its absorbance spectrum. Results in Figure 25 show a reduction of PL of both n1 and n4 parts, in comparison to their single flake emission. The PL emission of n1 flake is partially absorbed by n4 flake, whose PL intensity in the heterostructure is lower since the excitation power has been reduced by the partial absorption in the top n1 flake. Therefore, the absorption of n1 flake of the excitation

eliminates the gain in intensity of the n4 layer underneath. This experiment allowed us to establish the stack order looking for improving the n4 PL emission efficiency.

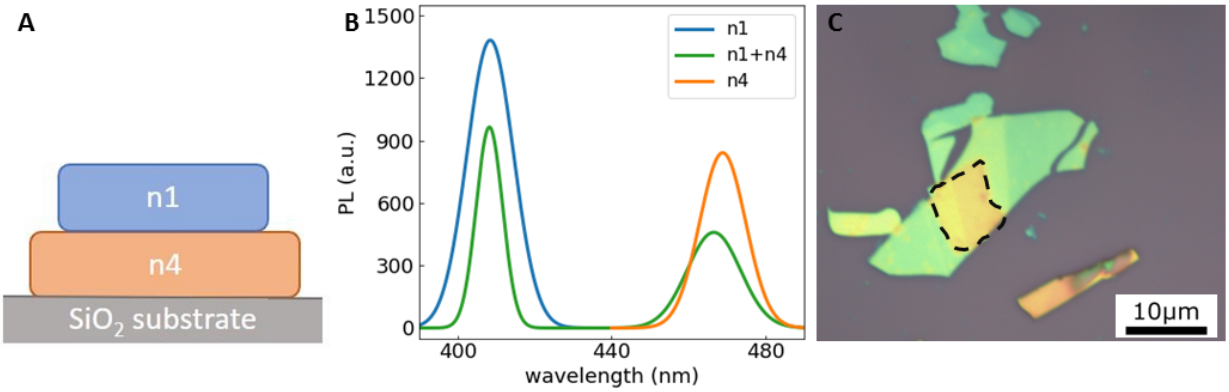

Figure 25: Analysis of a representative n4/n1 flakes heterostructure. (a) Order of the heterostructure. (b) PL emission of the heterostructure and the individual flakes. (c) Optical image.

3.3.2 Effect of an hBN barrier

Next, we repeated the same experiment for heterostructures n1/n4 flakes but including a hBN flake between the n1 and n4 flakes. We have to consider the following possible mechanisms:

1. Charge transfer. Charge carriers flow from the n1 flake to the n4 flake due to the band alignment.

2. Energy transfer. The n4 flake can be excited by the PL emission of the n1 flake, but this process cannot happen the other way round according to the band energy alignment. In practice, the n4 flake gets excited by a 'second light source', while n1 PL emission gets absorbed by n4 flake.

With an hBN barrier between the two compounds, we should block the possible charge transfer processes since hBN is an insulating material with large bandgap (see Fig. 26). Comparing the results of this type of heterostructures with the previous ones, we can calculate which mechanism is predominant.

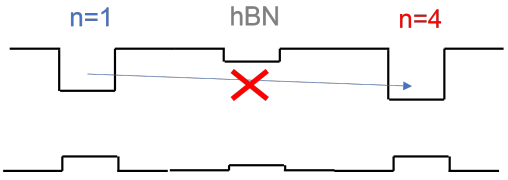

Figure 26: Charge transfer blocked by the hBN layer between the perovskite flakes.

From the results shown in Figure 27, we observe a similar behaviour than in the n1/n4 case. The PL emission intensity of n4 flake is enhanced and the one of n1 flake reduced and the enhancement achieved in this case is in the same order of magnitude. One should

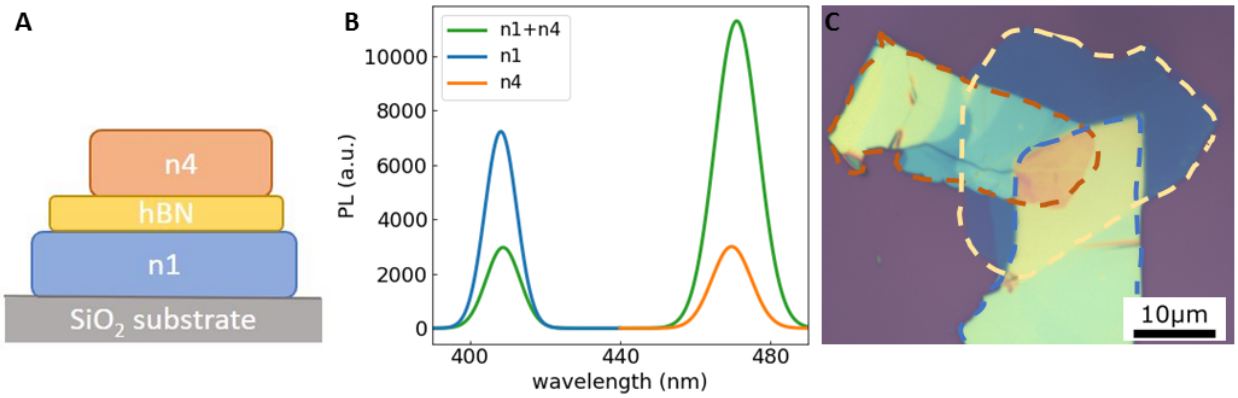

Figure 27: Analysis of a representative n1/hBN/n4 heterostructure. (a) Order of the heterostructure. (b) PL emission of the heterostructure and individual n1 and n4 flakes. (c) Optical image with highlighted limits of every component.

consider than in this case the PL intensity of the n1 flake used is higher. Therefore, an energy transfer between the flakes occurs.

Therefore, we can conclude that the use of hBN does not produce any change in the PL emission, nor in the n4 enhancement.

3.3.3 Effect of flake thickness

Lastly, we analysed the effect of the thickness of the perovskite flakes, regarding to the resulting photoluminescence emission.

Order of the heterostructure: n4/n1

To set up the experiment, we have made several heterostructures increasing the thickness of the n1 flake (which is on top) and keeping the same thickness for the n4 flake. We carried out the same PL measurements as before, and we observed that the thicker the n1 top flake is, the less n4 PL emission is obtained, see Table 3.

Table 3: Thickness of the n1 and n4 flakes forming the heterostructure and PL results in terms of the percentage difference compared to the PL emission of the uncovered part of the flake.

Thickness (nm)			PL change	
n4	n1	ratio	n4	n1
40	50	1-1.2	-64%	-31%
40	70	1-1.75	-80%	-25%
45	90	1-2	-86%	-27%

Therefore, we can argue that the thicker the top n1 flake is the more light it absorbs, and

the the more the intensity of the n4 flake emission decreases, although it is able to absorb part of the n1 flake PL emission.

Order of the heterostructure: n1/n4

We look for the relation between the thickness proportions and the PL intensity enhancement achieved in n4 flake at the heterostructure.

For this experiment we have prepared an heterostructure using two flakes with regions with different thickness forming terraces, see Image 28. With this sample, we can measure the change on PL emisision through the steps of any of the flakes (effectively varying its total thickness).

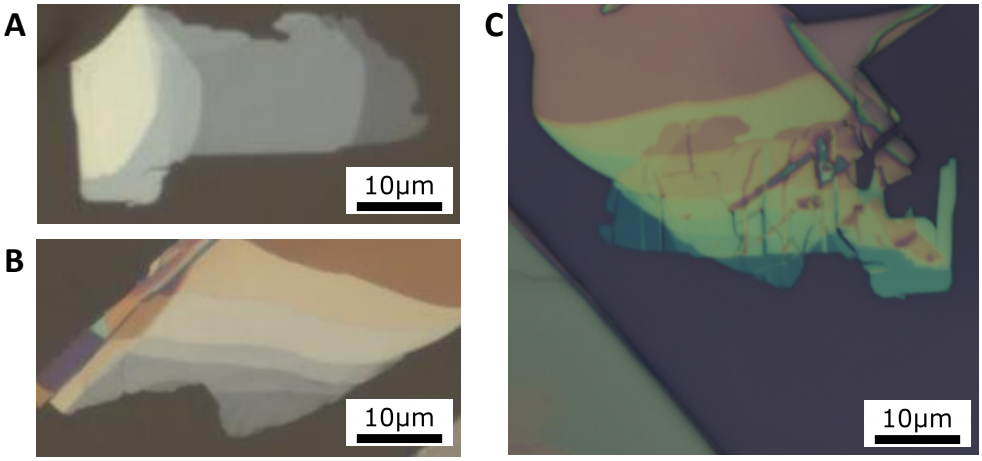

Figure 28: The n1/n4 heterostructure and the two flakes it is built of, (a) n4 layer (b) n1 layer, and (c) the resulting n1/n4 heterostructure.

First, we measured the PL emission through a direction where n4 flake stayed constant in thickness, while the thickness of n1 changes. We collected more than one set of data, and they are displayed on Figure 29 a-b. With this test, we can evaluate the behaviour of the n4 PL emission, as the thickness of that flake is constant. Results show that n4 PL intensity systematically increases as the n1 layer underneath is thicker.

Next, we measured the PL emission through other direction, that is, where n1 flake thickness remains constant and n4 flake thickness varies. Our sets of data are displayed on Figure 29 c-d. Results show that n1 flake PL intensity drops as the n4 layer on top thickens. This can happen due to the combination two factors: i) The thicker the n4 layer is the more light it blocks, both inwards and outwards, and also ii) a thicker n4 layer generates a larger energy transfer.

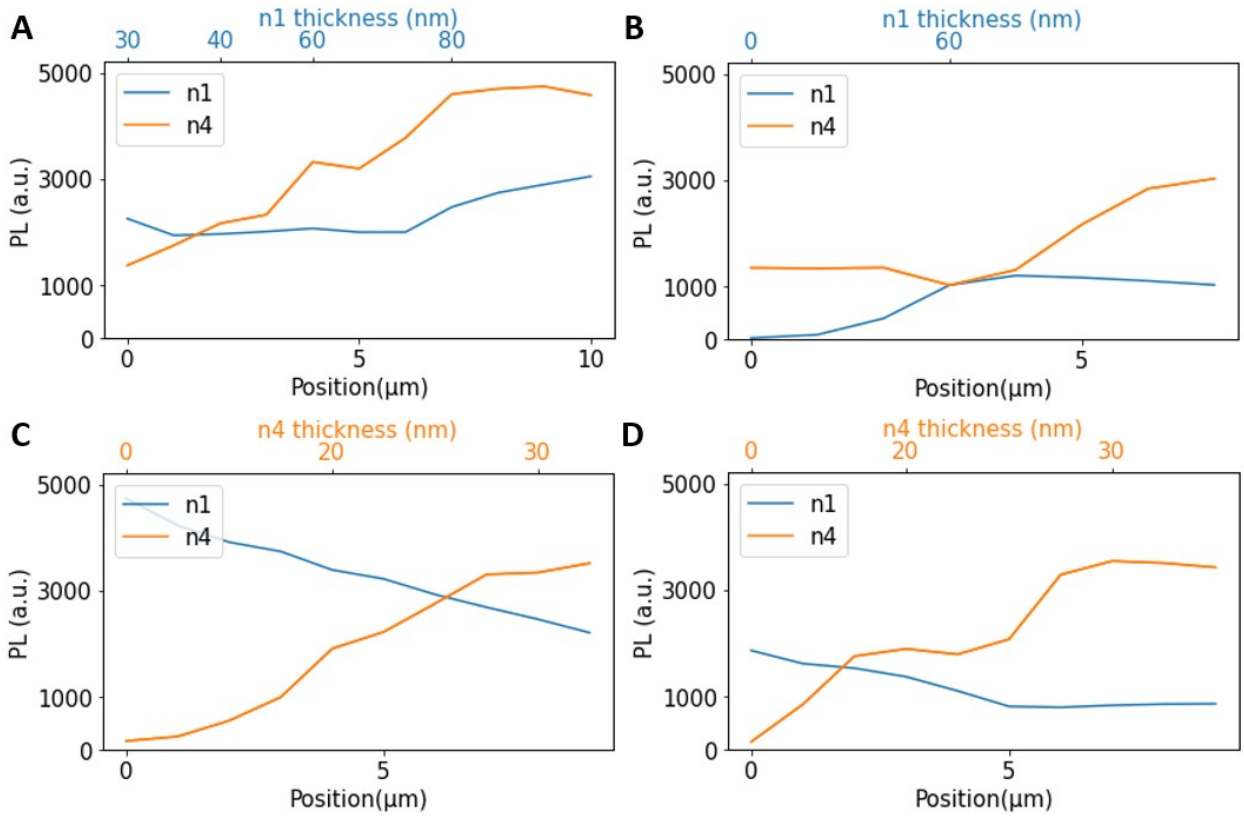

Figure 29: Photoluminescence intensity evaluation of the n1/n4 heterostructure. (a) n4 flake with constant thickness of 30nm and (b) n4 flake with constant thickness of 20nm. (c) n1 flake with constant thickness of 100nm and (d) n1 flake with constant thickness of 80nm.

4 Conclusions

Throughout this work, we have studied the optical properties of the layered metal-halide perovskite structures, concretely the photoluminescence emission.

First, we characterized the photoluminescence emission of the starting materials as bulk crystals and mechanically exfoliated flakes. From the experimental results obtained, we have demonstrated the tuning of the photoluminescence emission of 2D metal halide perovskites by changing the dimensionality, while there is no significant variation with the organic cation, (BA) and (PEA), or the thickness.

Next, we carried out a deep analysis on the ambient and light stability of perovskite flakes. Regarding to their atmosphere protection, we showed that the hBN encapsulation is a simple and effective method to achieve long-term stability, independently of the composition of the perovskites, and also well suited to device fabrication. However, this strategy is not valid for light protection.

Finally, with the fabrication of vertical heterostructures using as building blocks perovskite flakes with different dimensionality, we were able to further modulate the photoluminescence emission color and most important enhance the PL emission of one of the components. Moreover, placing a hBN flake between the perovskite flakes, we confirm that the mechanism occurring is an energy transfer from the perovskite with larger bandgap to the one with shorter bandgap. We also showed the effect of the thickness of the stacked flakes, and established the proper layer ordering to enhance the PL emission of the perovskite with shorter bandgap.

Acknowledgements

The experiments of this work were conducted in CIC nanoGUNE, the Basque Nanoscience Cooperative Research Center, Donostia, along the nanodevices research group.

References

[1] Ruoting Dong, Changyong Lan, Xiuwen Xu, Xiaoguang Liang, Xiaoying Hu, Dapan Li, Ziyao Zhou, Lei Shu, SenPo Yip, Chun Li, Sai-Wing Tsang, and Johnny C. Ho. Novel series of quasi-2D Ruddlesden–Popper perovskites based on short-chained spacer cation for enhanced photodetection. *ACS Applied Materials & Interfaces*, 10(22):19019–19026, 2018.

[2] Lingling Mao, Constantinos C. Stoumpos, and Mercouri G. Kanatzidis. Two-dimensional hybrid halide perovskites: Principles and promises. *Journal of the American Chemical Society*, 141(3):1171–1190, 2019.

[3] Jun Xing, Yongbiao Zhao, Mikhail Askerka, Li Na Quan, Xiwen Gong, Weijie Zhao, Jiaxin Zhao, Hairen Tan, Guankui Long, Liang Gao, Zhenyu Yang, Oleksandr Voznyy, Jiang Tang, Zheng-Hong Lu, Qihua Xiong, and Edward H. Sargent. Color-stable highly luminescent sky-blue perovskite light-emitting diodes. *Nature Communications*, 9(1):3541, 2018.

[4] Abd. Rashid bin Mohd. Yusoff and Mohammad Khaja Nazeeruddin. Low-dimensional perovskites: From synthesis to stability in perovskite solar cells. *Advanced Energy Materials*, 8(26):1702073, 2018.

[5] Matthew D. Smith, Bridget A. Connor, and Hemamala I. Karunadasa. Tuning the luminescence of layered halide perovskites. *Chemical Reviews*, 119(5):3104–3139, 2019.

[6] Dibyajyoti Ghosh, Debdipto Acharya, Laurent Pedesseau, Claudine Katan, Jacky Even, Sergei Tretiak, and Amanda J. Neukirch. Charge carrier dynamics in two-dimensional hybrid perovskites: Dion–Jacobson vs. Ruddlesden–Popper phases. *Journal of Materials Chemistry A*, 8(42):22009–22022, 2020.

[7] K. S. Novoselov, A. K. Geim, S. V. Morozov, D. Jiang, Y. Zhang, S. V. Dubonos, I. V. Grigorieva, and A. A. Firsov. Electric field effect in atomically thin carbon films. *Science*, 306(5696):666–669, October 2004.

[8] Robert C. Sinclair, James L. Suter, and Peter V. Coveney. Micromechanical exfoliation of graphene on the atomistic scale. *Physical Chemistry Chemical Physics*, 21(10):5716–5722, 2019.

[9] Andres Castellanos-Gomez, Michele Buscema, Rianda Molenaar, Vibhor Singh, Laurens Janssen, Herre S J van der Zant, and Gary A Steele. Deterministic transfer of two-dimensional materials by all-dry viscoelastic stamping. *2D Materials*, 1(1):011002, 2014.

[10] Bridget A. Connor, Linn Leppert, Matthew D. Smith, Jeffrey B. Neaton, and Hemamala I. Karunadasa. Layered halide double perovskites: Dimensional reduction of $Cs_2AgBiBr_6$. *Journal of the American Chemical Society*, 140(15):5235–5240, 2018.

[11] I. C. Smith, E. T. Hoke, D. Solis-Ibarra, M. D. McGehee, and H. I. Karunadasa. A layered hybrid perovskite solar-cell absorber with enhanced moisture stability. *Angewandte Chemie, International Edition*, 53(42):11232–11235, 2014.

[12] Jiabao Li, Jialong Duan, Xiya Yang, Yanyan Duan, Peizhi Yang, and Qunwei Tang. Review on recent progress of lead-free halide perovskites in optoelectronic applications. *Nano Energy*, 80:105526, 2021.

[13] Constantinos C. Stoumpos, Duyen H. Cao, Daniel J. Clark, Joshua Young, James M. Rondinelli, Joon I. Jang, Joseph T. Hupp, and Mercouri G. Kanatzidis. Ruddlesden–Popper Hybrid Lead Iodide Perovskite 2D Homologous Semiconductors. *Chemistry of Materials*, 28(8):2852–2867, 2016.

[14] Jun Hong Noh, Sang Hyuk Im, Jin Hyuck Heo, Tarak N Mandal, and Sang Il Seok. Chemical management for colorful, efficient, and stable inorganic-organic hybrid nanostructured solar cells. *Nano Letters*, 13(4):1764–1769, 2013.

[15] Kailiang Zhang, Yulin Feng, Fang Wang, Zhengchun Yang, and John Wang. Two dimensional hexagonal boron nitride (2D-hBN): synthesis, properties and applications. *Journal of Materials Chemistry C*, 5:11992–12022, 2017.

[16] C. Elias, P. Valvin, T. Pelini, A. Summerfield, C. J. Mellor, T. S. Cheng, L. Eaves, C. T. Foxon, P. H. Beton, S. V. Novikov, B. Gil, and G. Cassabois. Direct band-gap crossover in epitaxial monolayer boron nitride. *Nature Communications*, 10(1):2639, 2019.

[17] G. Cassabois, P. Valvin, and B. Gil. Hexagonal boron nitride is an indirect bandgap semiconductor. *Nature Photonics*, 10(4):262–266, 2016.

[18] Chil Hyoung Lee, Go Bong Choi, Eun Mi Kim, Jongho Lee, Jaegeun Lee, Hi Gyu Moon, Myung Jong Kim, Yoong Ahm Kim, and Tae Hoon Seo. Gas Barrier Performance of Hexagonal Boron Nitride Monolayers Grown on Copper Foils with Electrochemical Polishing. *Applied Sciences*, 11(10):4599, 2021.

[19] Letian Dou, Andrew B. Wong, Yi Yu, Minliang Lai, Nikolay Kornienko, Samuel W. Eaton, Anthony Fu, Connor G. Bischak, Jie Ma, Tina Ding, Naomi S. Ginsberg, Lin-Wang Wang, A. Paul Alivisatos, and Peidong Yang. Atomically thin two-dimensional organic-inorganic hybrid perovskites. *Science*, 349(6255):1518–1521, 2015.

[20] Emilio J. Juarez-Perez, Luis K. Ono, Maki Maeda, Yan Jiang, Zafer Hawash, and Yabing Qi. Photodecomposition and thermal decomposition in methylammonium halide lead perovskites and inferred design principles to increase photovoltaic device stability. *Journal of Materials Chemistry A*, 6:9604–9612, 2018.

[21] Dongxu Pan, Yongping Fu, Natalia Spitha, Yuzhou Zhao, Chris R. Roy, Darien J. Morrow, Daniel D. Kohler, John C. Wright, and Song Jin. Deterministic fabrication of arbitrary vertical heterostructures of two-dimensional Ruddlesden–Popper halide perovskites. *Nature Nanotechnology*, 16(2):159–165, 2021.